BMC Medical Genomics

RESEARCH

Open Access

Analysis of clinical phenotypes and genetic variations in two pedigrees affected with Weiss–Kruszka syndrome

Chunxiao Han[1,2,3], Changshui Chen[2*], Yuxin Zhang[1,2,3] and Haibo Li[1,2,3*]

Abstract

Background Weiss-Kruszka syndrome (WSKA) is a rare autosomal dominant syndrome characterized by multiple congenital anomalies caused by variants in the zinc finger protein 462 gene (ZNF462). About 40 cases of Weiss-Kruszka syndrome have been reported worldwide, and the aim of this study was to investigate the genetic causes of three patients from two Weiss-Kruszka syndrome family pedigrees with the aim of accumulating more data on the disease.

Objective To explore the clinical and genetic characteristics of two pedigrees with Weiss–Kruszka syndrome.

Methods The clinical data and family history of patients and family members of two pedigrees with Weiss–Kruszka syndrome were collected, and the pathogenic genes of the patients were analysed by whole-exon sequencing. Suspicious variants were verified by Sanger sequencing verification and bioinformatics prediction.

Results Proband 1 has developmental delay, autistic behaviour, and abnormal electroencephalogram results. WES revealed a classical heterozygous c.6696–2 A > C splice variant of the *ZNF462* gene, which was detected in neither parent. This position was conserved, and the variant was predicted to be deleterious. Minigene assays revealed that three types of aberrantly spliced mRNAs were produced. MRI of proband 2 suggested dysplasia of the corpus callosum with the formation of hemispheric cleft cysts, with a teardrop-like appearance in the lateral ventricle. WES revealed that a heterozygous c.4891 C > T:p. The Glu1631Ter nonsense variant of the *ZNF462* gene was inherited from her mother. According to the guidelines of the American Society of Medical Genetics and combined with its clinical manifestations, c.6696–2 A > C and c.4891 C > T:p. Glu1631Ter was determined to be a possible pathogenic variant.

Conclusion The c.6696-2 A>C and c.4891C > T:p.Glu1631Ter of the *ZNF462* gene likely underlies Weiss–Kruszka syndrome in children (foetus), which enriches the variant spectrum of Chinese patients with Weiss–Kruszka syndrome and provides a basis for prenatal diagnosis and genetic counselling.

Keywords Weiss–Kruszka syndrome, *ZNF462* gene, Whole-exome sequencing

*Correspondence:
Changshui Chen
chencs@139.com
Haibo Li
lihaibo-775@163.com
[1]The Central Laboratory for Birth Defects Prevention and Control, The Affiliated Women and Children's Hospital of Ningbo University, Ningbo 315010, China
[2]Ningbo Key Laboratory for the Prevention and Treatment of Embryogenic Diseases, The Affiliated Women and Children's Hospital of Ningbo University, Ningbo 315010, China
[3]Ningbo Key Laboratory of Genomic Medicine and Birth Defects Prevention, The Affiliated Women and Children's Hospital of Ningbo University, Ningbo 315010, China

Introduction

Weiss–Kruszka syndrome (WSKA) is a rare autosomal dominant syndrome characterized by multiple congenital anomalies resulting from a variant zinc finger protein 462 gene (ZNF462). The clinical characteristics of individuals with WSKA include a short nose with supination, downward-sloping blepharosphene, ptosis, atypical head shape, epidermal folds, arched eyebrows, and a minor developmental delay. Other clinical phenotypes that may be observed include hypotonia and feeding difficulties in approximately 50% of cases, prenatal elevation or closure of cranial sutures in 38% of cases, hypoplasia of the corpus callosum on brain imaging in 24% of cases, and structural heart defects in 21% of cases. Minor limb abnormalities are less common, occurring in approximately 25% of cases [1]. Importantly, the majority (approximately 95%) of WSKA cases are de novo, meaning that they occur spontaneously and are not inherited from parents. However, a small percentage of cases are familial and exhibit significant heterogeneity [2]. Currently, approximately 40 cases of WSKA have been reported worldwide, highlighting the rarity of this syndrome. Notably, only two Weiss–Kruszka syndrome families have been reported in China [3, 4]. Given the scarcity of cases and limited understanding of WSKA, the aim of this study was to investigate the genetic causes underlying the clinical manifestations of autism with EEG abnormalities and foetal hypoplasia of the corpus callosum in two specific family pedigrees.

Methods

Sample Collection

The relevant clinical data of the probands, including medical history and family history, were collected. Five millilitres of venous blood was extracted from the patient and parents, 0.5 mg of foetal medial thigh muscle tissue was clipped, and DNA was extracted for whole-exome sequencing via the QIAamp DNA Blood Mini Kit (Qiagen, Germany).

Trio whole-exome sequencing analysis

Whole-exome sequencing analysis High-throughput sequencing (Nova seq6000, Illumina, USA) was performed after hybridization capture and enrichment of whole-exome DNA using the Nano-WES probe (Twist Bioscience, USA), and the quality standards of the sequencing data were as follows: average sequencing depth of 100×~150×, quality of the data table of Q20≥85% and Q30≥80%. The raw sequencing data were compared with human reference gene sequences, and GATK and VarScan software were used to identify and annotate the variants. The 1000 Genomes (http://gnomad-sg.org), dbSNP (http://www.ncbi.nlm.nih.gov/SNP/), gnomAD (http://gnomad-sg.org/), HGMD (https://www.hgmd.cf.ac.uk/ac/validate.php), ClinVar (https://www.ncbi.nlm.nih.gov/clinvar/) and other databases were used to screen for possible pathogenic variants.

Table 1 Primer sequences for Sanger sequencing

Variation Position	Primer Sequence(5′→3′)
c.6696–2 A > C	F: GCACTTGGACATATATAACGGGT R: TAGAGGCAGAGAGGACAGCG
c.4891 C > T	F: GTGACCGCTGAGGACTTT R: CTCGGACATTATTGTGCTTG

Table 2 Minigene primer sequences for Sanger sequencing

Variation Position	Primer Sequence(5′→3′)
pcMINI-F	ACTTAAGCTTatgagtgggctttggggtggccggtt
pcMINI-R	TAGAAGGCACAGTCGAGG
pcMINI-N-F	CTAGAGAACCCACTGCTTAC
pcMINI-N-R	GCCCTCTAGActggtcattccggctc

Sanger sequencing and family analysis

Sanger sequencing was performed to validate the DNA of the affected and family members, and primers were designed for the heterozygous missense variant site in the *ZNF462* gene using Premier 5.0 software (Table 1). The PCR products were purified and subjected to sequencing via PCR with bigdyeTerinatorv3.1 and finally sequenced on an ABI-3500DX.

Predicting splicing disruptions

Two visualization software packages, the Human Splicing Finder (HSF) v3.0 (https://www.genomnis.com/accesshsf) (Desmet et al., 2009) and Splicing AI (https://spliceailookup.broadinstitute.org/), were employed for the online analysis of splice variant harmfulness. These software packages were utilized specifically to predict splice variants and assess the potential strength of new/cryptic splicing sites in the *ZNF462* gene variant.

Minigene

Two vector models, pcMINI and pcMINI-N, were utilized to construct a minigene (NM_021224.6:c.6696–2 A > C). The pcMINI-wt/mut sequence was amplified via PCR using the primers pcMINI-F and pcMINI-R. Similarly, the pcMINI-N-wt/mut sequence was amplified using the primers pcMINI-N-F and pcMINI-N-R. Following amplification, the wild-type and mutant minigene sequences were separately inserted into the pcMINI and pcMINI-N vectors. In total, four recombinant vectors were then transfected into the HeLa and 293T cell lines. After 48 h of transfection, a total of eight samples were collected for RNA extraction. The specific sequences of primers used can be found in Table 2. For further information on the minigene vector construction strategy, please refer to the Supplementary Material (Table S2).

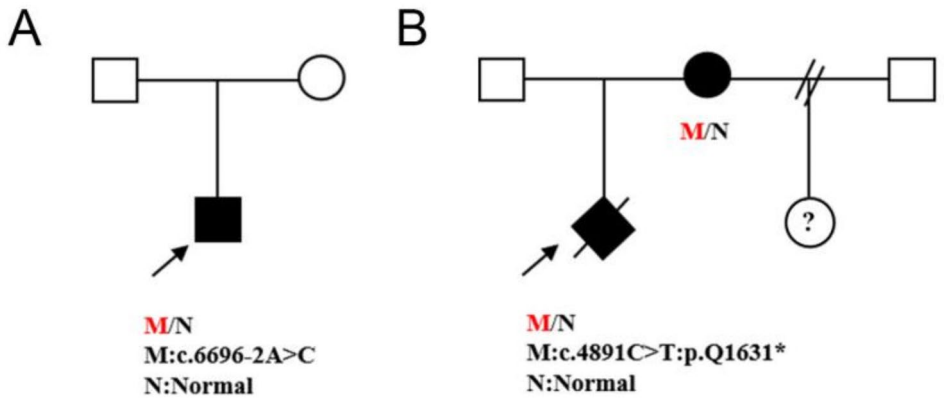

Fig. 1 Pedigree of two Weiss–Kruszka syndromes. **A** Family tree of pedigree 1. **B** Family tree of Pedigree 2

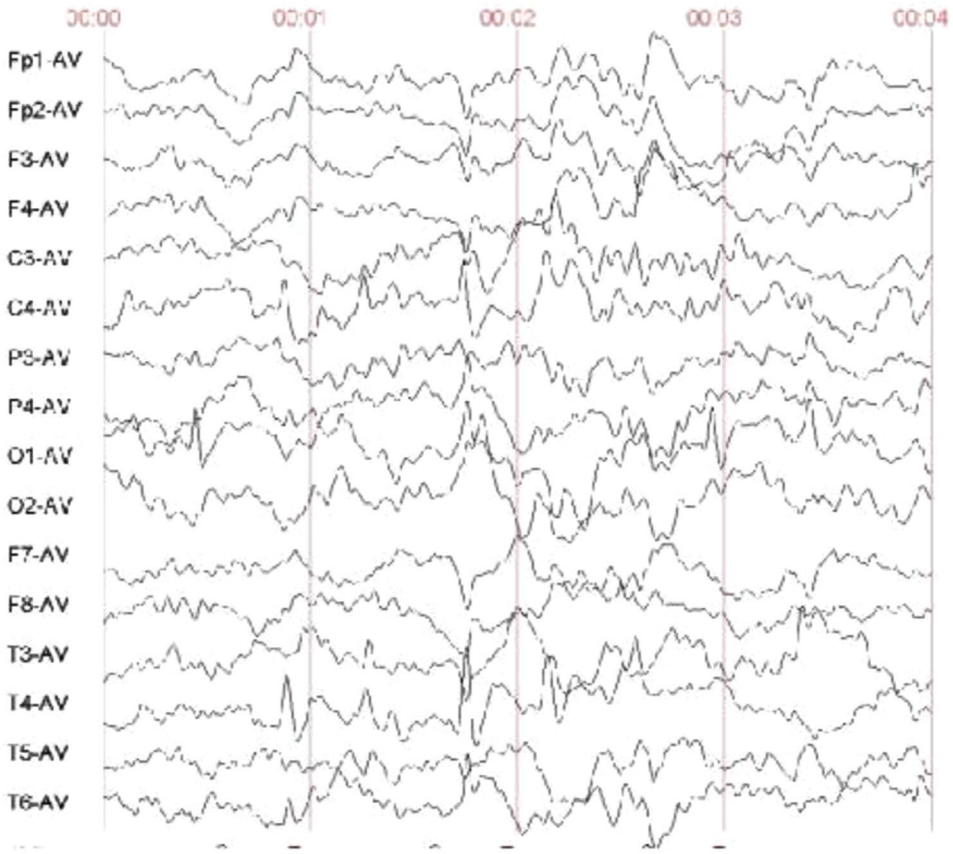

Fig. 2 EEG of Proband 1. The results revealed that in the right central and thick temporal regions, the left occipital and middle temporal regions had many low– to medium-amplitude spines, spines and slow waves, the left and right sides were out of sync, and the right side was on. The EEG power changed with increasing δ power

Results

Clinical reports

The proband in Family 1 (Fig. 1A) is a 6-year-old male child who presented with developmental delay and speech and communication disorders and was clinically diagnosed with Asperger syndrome (AS). The chromosome copy number of the proband is arr(1–22)x2,(XY)x1. Physical examination revealed facial manifestations of ptosis, whereas hearing and MRI findings were within normal ranges. Electroencephalogram (EEG) results demonstrated the presence of multiple low–moderate amplitude spikes and slow spikes in the right central and faithful temporal regions, as well as in the left occipital and mesial temporal regions, with left–right asynchrony. The spikes were more pronounced on the right side. EEG power analysis revealed increased δ power (Fig. 2). There

was no family history, the parents were nonconsanguineous, and the phenotype was not abnormal.

In Family 2 (Fig. 1B), a 37-year-old woman referred to a prenatal centre underwent an ultrasound examination, which revealed the absence of the corpus callosum in the foetus. Prior to this pregnancy, the woman had undergone two induced abortions with her ex-husband. This current pregnancy is her fourth, and she already has a daughter from her previous marriage, who displayed no obvious abnormalities without genetic testing. This pregnancy is progressing naturally, with no abnormalities detected in the foetal neck's transparent layer via ultrasound examination (NT). Furthermore, noninvasive prenatal testing (NIPT) revealed a low-risk profile and the absence of any predisposing conditions, such as diabetes or hypertension, during pregnancy. However, at the 24-week mark, a three-dimensional ultrasound of the foetus unexpectedly indicated the presence of a development that had not been anticipated earlier. However, ultrasound at 24^{+5} weeks of pregnancy revealed no clear septum in the foetus at 24+5 weeks of gestation (Fig. 3A). Further imaging via MRI confirmed the agenesis of the corpus callosum (Fig. 3B), as well as dilated bilateral ventricles that were parallel in alignment. Additionally, the posterior part of the bilateral ventricles had a rounded teardrop shape, and the third ventricle appeared enlarged, with the upper table located in a saccadic position between the bilateral ventricles (Fig. 3C). Foetal cardiac ultrasound revealed no abnormalities. The current husband of the pregnant woman has no biological ties to her, and she presents with ptosis, a noticeable facial manifestation. However, her auditory functions and MRI scan results revealed no abnormalities. Furthermore, her echocardiography examination was unremarkable, indicating no issues with her heart's structure or function. Following genetic counselling, the mother made the decision to terminate the pregnancy at 25^{+1} weeks. With the consent of the family, foetal medial thigh muscle tissue and peripheral blood samples from the parents were collected for whole-exome sequencing analysis to investigate the family's genetic line.

Sequencing and microarray results

The results of exome sequencing revealed that Proband 1 presented a de novo variant, c.6696–2 A>C, in the *ZNF462* gene, specifically, a classic splice site variant. This particular variant, which is not found in the gnomAD database (PM2_Supporting), may have implications for mRNA splicing and protein function (PVS1). Furthermore, Sanger sequencing results indicated that the parents of Proband 1 had wild-type sequences (PM6), suggesting that the variant is likely a de novo variant (Fig. 4A). Based on the ACMG standards and guidelines, this variant was assessed as pathogenic. For Proband 2, the chromosome copy number of this pregnancy was arr(1–22)x2,(XY)x1. Exome sequencing revealed a heterozygous nonsense variant, c.4891 C>T:p. Glu1631Ter on the *ZNF462* gene. This variant replaces base 4891 of the cDNA from a C to a T, causing codon 1631 to change from encoding glutamine to a termination codon. Consequently, this alteration may lead to protein truncation or degradation via nonsense-mediated mRNA decay, ultimately affecting protein function (PVS1). Like in Proband 1, this variant is not reported in the gnomAD database (PM2_Supporting). Sanger sequencing revealed that Proband 2 was inherited from her mother, whereas her father had the wild type (Fig. 4B). In accordance with the applicable ACMG standards and guidelines, this variant was assessed as a possible pathogenic variant.

Bioinformatics predictions

According to the SpliceAI prediction tools, the variant c.6696–2 A>C was determined to be deleterious and potentially capable of inducing abnormal splicing. This finding is supported by Table 3. Additionally, the analysis conducted via HSF predictions indicated that the

Fig. 3 Proband 2 ultrasound and MRI findings. **A** Ultrasound revealed an intracranial hyaline septal cavity defect. **B** MRI image suggestive of a foetal corpus callosum defect. **C** MRI suggested interhemispheric fissure cysts

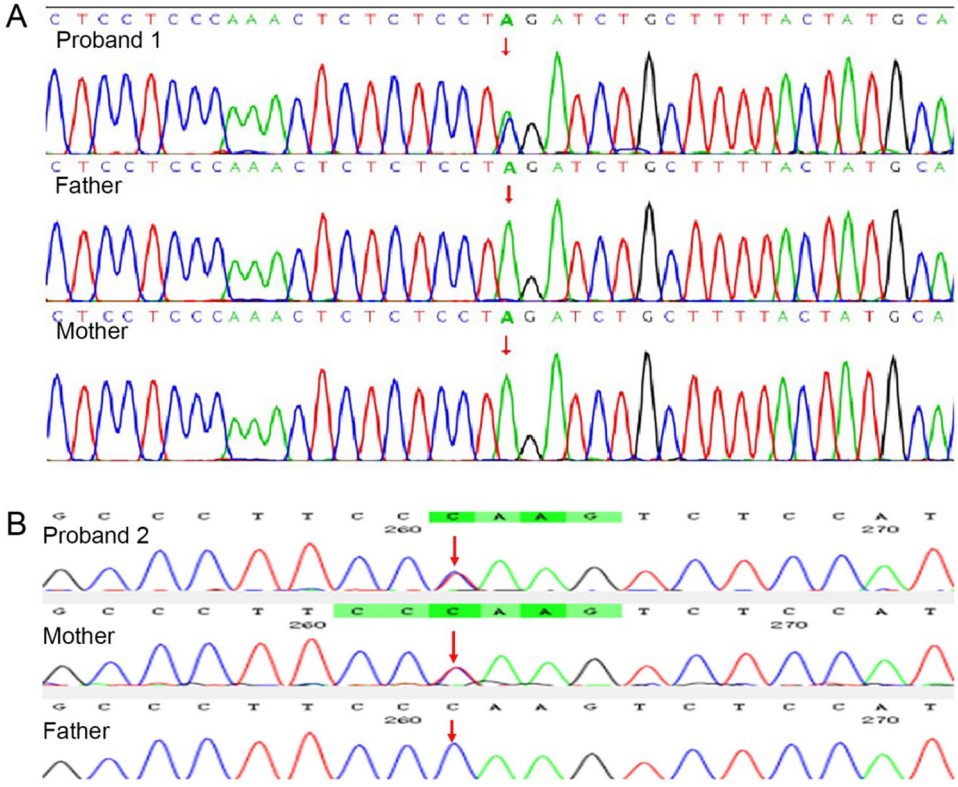

Fig. 4 Sanger sequencing results for two family pedigrees. Genetic testing revealed that Proband 1 had a de novo variant in the NM_021224.6:c.6696–2 A > C *ZNF462* variant and that the parents carried the wild-type gene. **B** Genetic testing revealed that the NM_021224.6:c.4891 C > T:p.Glu1631Ter *ZNF462* variant in Proband 2 was inherited from the mother. The father carried the wild-type gene

Table 3 Functional prediction of the variant via SpliceAI

Variant	Gene	△Type	△Score	Position
NM_021224.6(ZNF462):c.6696–2 A > C	ZNF462	Acceptor Loss	0.96	2 bp
		Donor Loss	0.48	138 bp
		Acceptor Gain	0.20	-114 bp
		Donor Gain	/	/

Table 4 Human splicing finder v3.0 predicted the c.6696–2 A > C variant of the ZNF462 gene

HSF algorithm	HSF matrix
position	Chr9:106974125
Sequence Reference	ACTCTCTCCTAGAT
Sequence variant	ACTCTCTCCTCGAT
Score Reference	81.22
Score variant	53.35
Delta	-34.35%
Results	Site Donor Broken

Abbreviations: HSF, human splicing finder

c.6696–2 A > C variant could disrupt the wild-type donor site and potentially give rise to new variable splice sites. These results are summarized in Table 4.

Minigene experiment

Minigene in vitro assays revealed that the variant c.6696–2 A > C affects the normal splicing of gene mRNA, and the results were consistent between the two sets of vectors, pcMINI and pcMINI-N. Three types of aberrant splicing exist after the variant: ① the intron 8 right side lagging 116 bp; ② the exon 9 left side deletion of 26 bp; ③ and exon 9 jumping (Figs. 5 and 6).

The right side of intron 8 retains 116 bp in the cDNA representation as c.6695_6696insCCCCACAAGCAGGAGAGCCG-CACTTGGACATATATAACGGGTTTGCCAGCAG-GAAATGTGAAAATGCAATGATCCCTGGTTACAC-GCATCACCTCTCCTCCCAAACTCTCTCCTCG p. Lys2232Asnfs*13. ② Exon 9 had a 26 bp deletion in cDNA: c.6696_6721del p.Lys2232Asnfs*31. ③ Exon 9 jumps in the cDNA representation: c.6696_6832del p.Ser2233Argfs*7.

Discussion

Weiss–Kruszka syndrome is a rare genetic disorder that was initially documented by Ramocki [5]. Most individuals with WKSA exhibit distinct facial characteristics, with ptosis being the most prevalent clinical feature, which is observed in approximately 84% of cases. Other facial abnormalities commonly observed include downward-sloping blepharophimosis, arched eyebrows, a medial canthus, and a short arched nose. Furthermore,

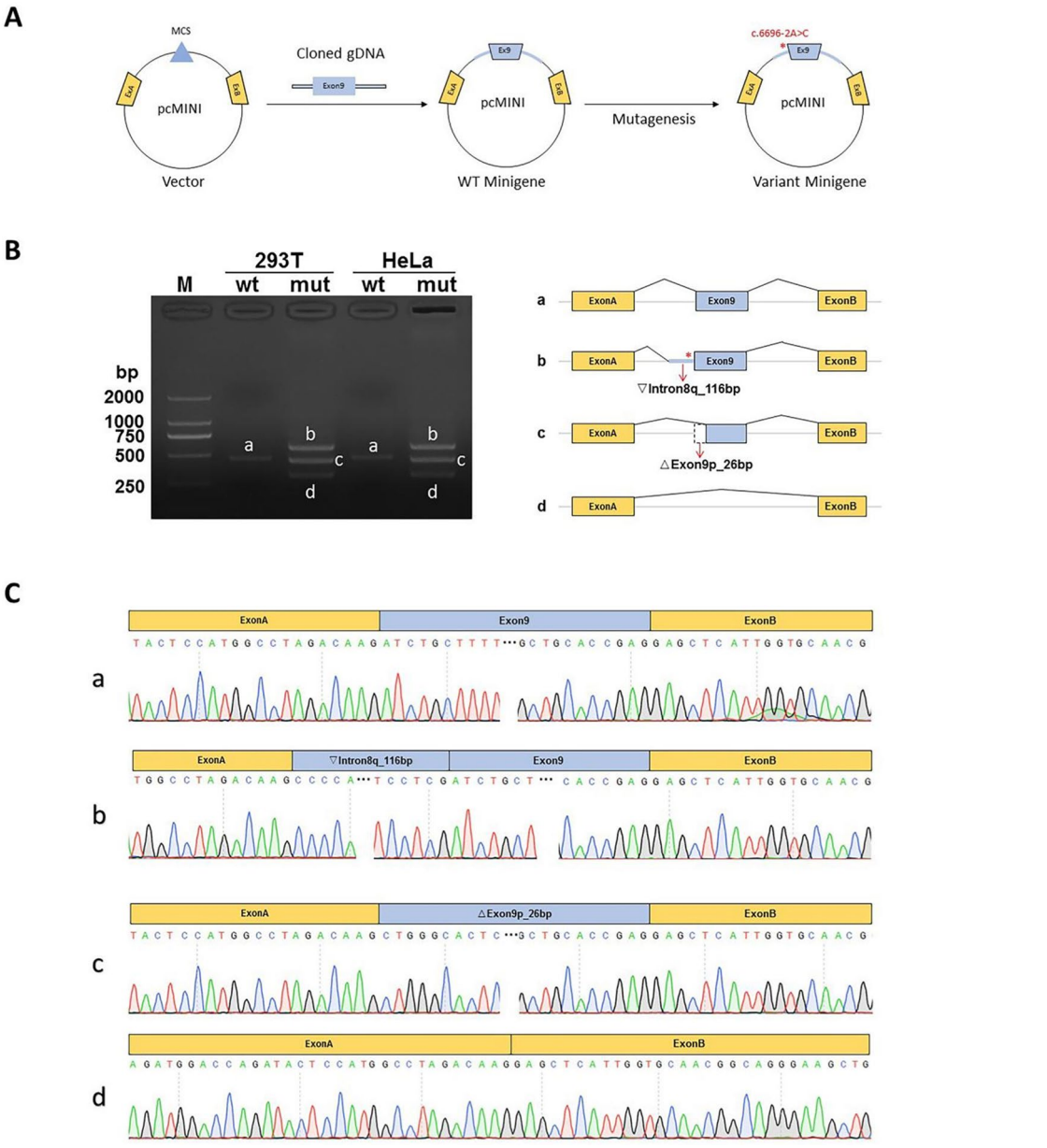

Fig. 5 pcMINI vector construction for the gene *ZNF462* c.6696–2 A > C. Minigene construction strategy. **B** Agarose gel electrophoresis revealed the presence of a single band corresponding to the wild type, and three distinct bands corresponding to the mutants b, c, and d. **C** Splice variant sequencing results in HeLa and 293T cells, with a wild type in the splice band, b: Intron8 right side lagging 116 bp, c: Exon 9 left side deletion of 26 bp, and d: Exon 9 jumping. Red * indicates the position of the variant

approximately 75% of patients experience mild developmental delays, with speech delays being the most frequently reported, which affect approximately 42% of individuals. Approximately one-third of WKSA patients also receive a diagnosis of autism spectrum disorder. Other clinical features of WKSA include cardiovascular abnormalities in 21% of cases, hearing loss or outer ear abnormalities in 51% of cases, feeding difficulties in 45% of cases, and abnormal development of the corpus callosum in 28% of cases [3, 6, 7]. According to data from the PubMed database, no more than 40 cases of individuals with WKSA have been reported as of January 2024. In China, only three cases of WKSA have been reported, all of which are from two family lines. These three patients also exhibit facial characteristics such as ptosis, arched eyebrows, and a short-arched nose. Moreover, Zhou et al. documented the case of a male child with WKSA who displayed clinical signs of attention deficit hyperactivity disorder and complete growth hormone deficiency [4]. A recent groundbreaking study conducted by Constantinou et al. proposed a potential link between WSKA and the autoimmune condition known as systemic lupus

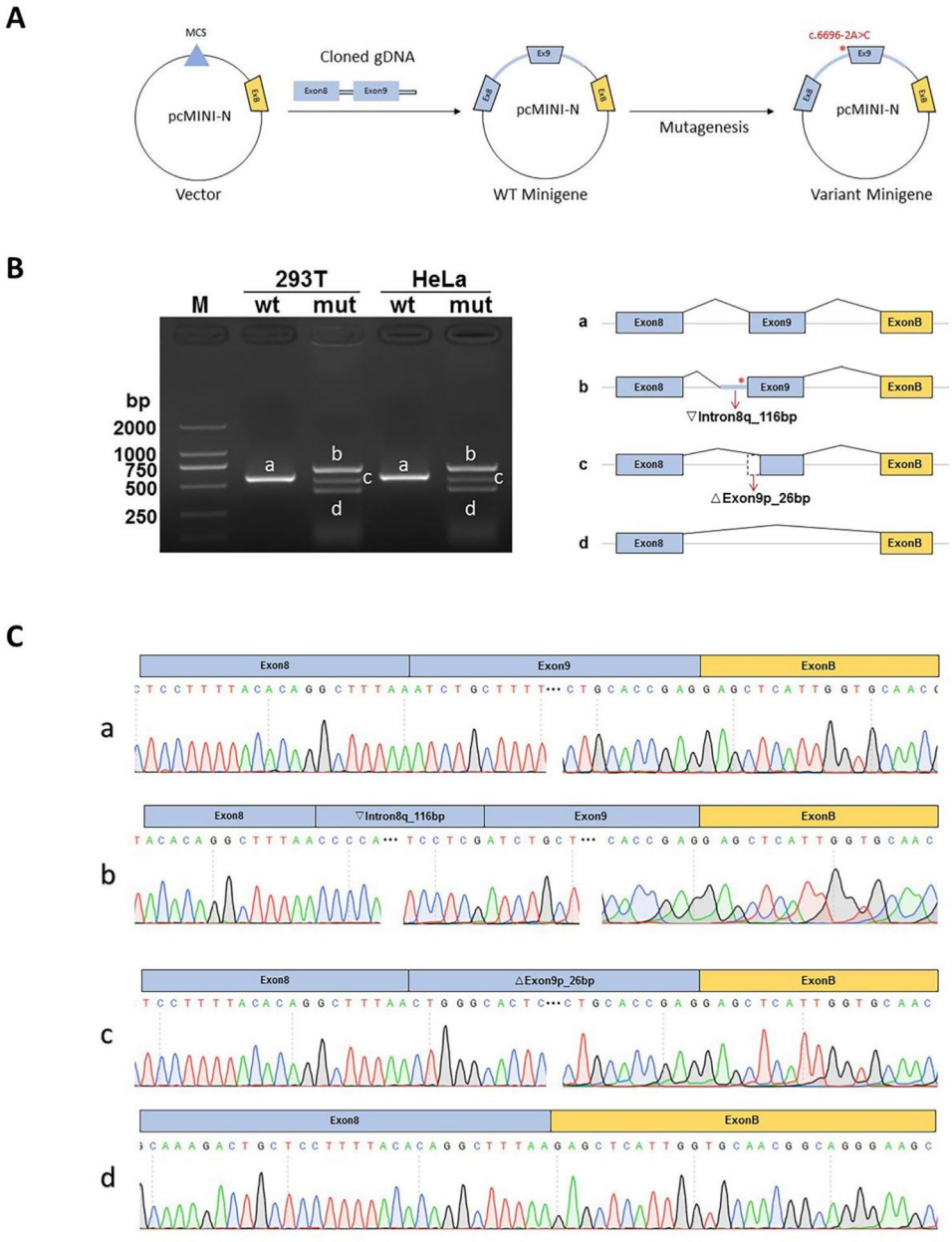

Fig. 6 pcMINI-N vector construction in the *ZNF462* gene c.6696–2 A > C. **A** Minigene construction strategy. **B** Agarose gel electrophoresis revealed the presence of a single band corresponding to the wild type and three distinct bands corresponding to the mutants b, c, and d. **C** Splice variant sequencing results in HeLa and 293T cells, with a wild type in the splice band, b: Intron8 right side lagging 116 bp, c: Exon9 left side deletion of 26 bp, and d: Exon9 jumping. Red * indicates the position of the variant

erythematosus (SLE), underscoring the paramount importance of exploring the role of chromatin remodelling in the intricate pathogenesis of not only SLE but also a broad spectrum of autoimmune and autoinflammatory disorders [8]. Additionally, Zhao et al. reported the case of a a male child with WKSA who inherited the condition from his father and was born with an arterial conduit arterial ductus arteriosus. Both the child and his father were hearing impaired [3].

The WES results suggested that the heterozygous classical splice site variant c.6696–2 A>C in the *ZNF462* gene, which was suggested to be de novo by Sanger sequencing, was located in intron 8, the 23rd C2H2 zinc-finger construct, which may affect the shear position of the mRNA, and the function of the next four zinc-finger structural domains may be affected. We used predictive software programs to analyse the variant, which revealed that the wild-type donor site may be disrupted, leading to a premature termination codon. The in vitro minigene

experiment confirmed this prediction; after cloning and sequencing, the splicing variant produced three mRNA products that may result in truncated proteins. The WES results suggested that Proband 2 had a heterozygous nonsense variant, c.4891 C>T: p.Q1631*, in the *ZNF462* gene, which was inherited from the mother. This mutation leads to a change in codon 1631 from a glutamine to a stop codon and may result in protein truncation or nonsense-mediated mRNA degradation; neither variant has been reported. As of January 2023, the HGMD database contains 39 missense/nonsense variants and 2 splice variants in the *ZNF462* gene, approximately 80% of which are located in exon 3 (https://www.hgmd.cf.ac.uk/ac/all.php). The *ZNF462* gene is located on chromosome 9q31.2, consists of 13 exons, encodes 2506 amino acids, has 27 C2H2 zinc finger structures, and is involved in the transcriptional regulation and chromosomal remodelling of zinc finger proteins by binding to DNA molecules. Zinc finger proteins are highly conserved in most mammals, are localized in the nucleus, play important roles in vertebrate models of embryonic development, and are widely expressed in a variety of human tissues [9–11]. The gene was first identified in a patient with a reciprocal translocation t(2;9)(p24;q32), where chromosomal rearrangements resulted in disruption of the genes *ZNF462* and *ASXL2* [5]. Eberl et al. found that the *ZNF462* protein is involved in heterochromatin formation and modification by binding to HP1α and H3K9me3 in histone peptides from mouse brain, kidney, and testis tissues [12]. Yelagandula et al. suggested that aberrant activation of lineage nonspecific genes in the neuronal lineage underlies ZNF462-associated neurodevelopmental pathology [13]. Masse et al. reported disruption of the pericentric structural domain and redistribution of the HP1α protein in *ZNF462* knockout pluripotent mouse cells and that *ZNF462* contributes to the maintenance of heterochromatin in pluripotent cells [14]. Zhou et al. reported via gene ontology enrichment analysis that the protein *ZNF462* and its interacting proteins ASXL2, VPS13B, and VAX1 may form a protein complex important for development, and they suggested that the interaction of the gene *ZNF462* with paired genes may be related to the pathogenic mechanism of Weiss–Kruszka syndrome [4]. Wang et al. reported that *ZNF462* -/- mice undergo prenatal death, and compared with wild-type ZNF462 +/- mice, *ZNF462* +/- mice exhibit reduced *ZNF462* expression, postnatal brain developmental delay and anxiety-like behaviour with excessive self-grooming [15].

Proband 1 in this study was clinically diagnosed with Asperger syndrome (AS), a genetic disorder characterized by verbal communication disorders, motor developmental delay, and ptosis. These symptoms align with the clinical phenotype of Weiss–Kruszka syndrome. An electroencephalogram (EEG) was performed on Proband 1, revealing multiple low–moderate amplitude spikes, spikes, and slow waves in regions such as the right central and faithful temporal regions and the left occipital and mesial temporal regions. These abnormalities occurred paroxysmally and exhibited left–right asynchrony. Additionally, increased δ-power was observed in the electroencephalographic power. Notably, the presence of EEG abnormalities in WSKA patients has not been reported previously. Kruszka conducted a comprehensive review of 24 patients with WSKA and reported that 33% (8/24) of them were diagnosed with autism spectrum disorders [1]. However, no records concerning EEG abnormalities were mentioned in these cases. A male child was reported to have a transcoding variant in the *ZNF462* gene. He presented clinically with delayed speech and motor development and experienced four dysarthria seizures at the age of 7 years. However, no abnormalities were observed in his EEG or MRI results [2]. EEG abnormalities are considered one of the neurobiological causes of autism, with studies indicating that 30–80% of children with autism spectrum disorder (ASD) exhibit concurrent EEG abnormalities [16]. In a Chinese study, EEG was conducted on 35 children with ASD, 6.3% (4/35) of whom displayed slow wave activity in the EEG background, whereas the remaining children did not show any specific changes [17]. Proband 1 was clinically diagnosed with ASD, and the syndrome belongs to the ASD subtype. EEG objectively reflects the brain function of children with ASD to some extent. These findings enrich the clinical phenotype of WSKA, but more case data are needed to further support these findings. Proband 2 underwent cranial MRI, which revealed hypoplasia of the corpus callosum. Sanger sequencing revealed that this variant was inherited from the mother, who, interestingly, was not found to have abnormalities on brain MRI or cardiac ultrasound. The mother showed only a peculiar facial appearance with droopy eyelids and no auditory abnormalities. Families afflicted with WKSA syndrome who have reported instances of genetic variation from their parents are scarce, with only two comprehensive sets of family data available to date. Zhao et al. reported the case of a boy with WKSA who inherited the disorder from his father and was born with ductus arteriosus. Both the child and his father were hearing impaired [3]. Another study identified six family pedigrees of Weiss–Kruszka syndrome, one of which included 4 generations consisting of 5 patients, including a 2-year-old sister, father, grandmother, and great grandfather. Only the 2-year-old sister exhibited agenesis of the corpus callosum, whereas the other patients had normal cranial MRI results [2]. This consistency with the findings reported in this study for Family 2 implies potential phenotypic heterogeneity at identical loci of variation among patients with Weiss–Kruszka syndrome. Therefore, we conducted

a follow-up with the grandparents of Proband 2. Based on the family's account, the pre-witness's grandparents exhibited no apparent abnormalities. Unfortunately, the family declined to undergo Sanger sequencing, a validation process that could have provided us with more intricate genetic insights. Nevertheless, analysing the existing clinical data and genetic findings reveals profound phenotypic heterogeneity within Family 2 regarding WKSA. However, given the scarcity of reported cases, a more comprehensive understanding of WKSA phenotypic diversity necessitates additional data support. Furthermore, in this study, both Proband 1 and Proband 2 carried different variant of the *ZNF462* gene. Interestingly, they both manifested different types of neurological abnormalities clinically. These findings suggest the possible involvement of the *ZNF462* gene in transcriptional regulation during embryogenesis, which affects neural crest migration and brain development. Therefore, the findings should be interpreted with caution.

Nonetheless, several potential limitations of our study should be noted. First, the presence of significant clinical phenotypic heterogeneity in family 2 is rare in previous reports, the heterozygosity for *ZNF462* gene has been reported in only 1 family in the past [2], which has been mentioned in the Discussion. Unfortunately we were unable to obtain genetic information from the grandparents of the proband 2, which hinders further research on the heterogeneity of hereditary WSKA. Second, we only functionally validated the variant in the *ZNF462* gene c.6696–2 A>C in proband 1 at the cellular level, demonstrating that the shear variant did affect RNA expression, but did not functionally validate the variant at the protein levels, so more research is needed to determine whether the shear compilation affects protein expression.

In summary, our study identified the presence of ZNF462 gene variants as a possible causative agent of Weiss-Kruszka syndrome in two affected probands by using whole exome sequencing (WES). This study not only enriches the spectrum of ZNF462 gene variants, but also provides an important basis for accurate diagnosis and genetic counseling for the two families affected by this rare genetic disorder.

Supplementary Information

The online version contains supplementary material available at https://doi.org/10.1186/s12920-024-02035-x.

Supplementary Material 1

Supplementary Material 2

Acknowledgements
We thank the patient and her family for participating in this study.

Author contributions
CH designed the study. YZ helped with clinical information. CH wrote the paper. CC and HL revised the manuscript critically. All authors read and approved the final manuscript.

Funding
This study was supported by the Ningbo Top Medical and Health Research Program (20220405), the Municipal Public Welfare Project of Ningbo (2022S035), the Ningbo Science and Technology Project (2023Z178), and Key Technology Breakthrough Program of Ningbo Sci-Tech Innovation YONGJIANG 2035 (2024Z221).

Data availability
The details of the variants c.6696–2 A> C, c.4891 C> T(p.Glu1631Ter) and analyzed in this study have been deposited into the ClinVar database (https://www.ncbi.nlm.nih.gov/clinvar/) with the accession number SCV005331508 and SCV005331509.

Declarations

Ethics approval and consent to participate
This study was approved by the Ethics Committee of Ningbo Women and Children's Hospital (EC2020-048). All methods were carried out in accordance with the relevant guidelines and regulation. The informed consent to participate was obtained from all of the participants and parents/legal guardians of minors.

Consent for publication
All the participants and the legal guardians/parents of minors gave written informed consent for their personal or clinical details along with any identifying images to be published in this study.

Competing interests
The authors declare no competing interests.

Received: 31 January 2024 / Accepted: 21 October 2024
Published online: 05 November 2024

References

1. Kruszka P, Hu T, Hong S, Signer R, Cogne B, Isidor B, et al. Phenotype delineation of ZNF462 related syndrome. Am J Med Genet A. 2019;179(10):2075–82.
2. Weiss K, Wigby K, Fannemel M, Henderson LB, Beck N, Ghali N, et al. Haploinsufficiency of ZNF462 is associated with craniofacial anomalies, corpus callosum dysgenesis, ptosis, and developmental delay. Eur J Hum Genet. 2017;25(8):946–51.
3. Zhao S, Miao C, Wang X, Lu Y, Liu H, Zhang X. A nonsense variant of ZNF462 gene Associated with Weiss-Kruszka Syndrome-Like manifestations: a Case Study and Literature Review. Front Genet. 2022;13:781832.
4. Zhou Y, Liu J, Wu S, Li W, Zheng Y. Case report: a heterozygous mutation in ZNF462 leads to growth hormone deficiency. Front Genet. 2022;13:1015021.
5. Ramocki MB, Dowling J, Grinberg I, Kimonis VE, Cardoso C, Gross A, et al. Reciprocal fusion transcripts of two novel Zn-finger genes in a female with absence of the corpus callosum, ocular colobomas and a balanced translocation between chromosomes 2p24 and 9q32. Eur J Hum Genet. 2003;11(7):527–34.
6. Brady L, Ballantyne M, Duck J, Fisker T, Kleefman R, Li C, et al. Further characterization of the 9q31 microdeletion phenotype; delineation of a common region of overlap containing ZNF462. Mol Genet Genomic Med. 2023;11(3):e2116.
7. Gonzalez-Tarancon R, Salvador-Ruperez E, Miramar Gallart MD, Barroso E, Diez Garcia-Prieto I, Perez Delgado R, et al. A novel mutation in the ZNF462 gene c.3306dup; p.(Gln1103Thrfs*10) is associated to Weiss-Kruszka syndrome. A case report. Acta Clin Belg. 2022;77(1):118–21.
8. Constantinou M, Lampi M, Parperis K, Neocleous V, Fanis P, Phylactou L, et al. A novel pathogenic variant in ZNF462 gene associated with Weiss-Kruszka syndrome and systemic lupus erythematosus. Rheumatology (Oxford). 2023;62(8):e249–50.

9. Lek M, Karczewski KJ, Minikel EV, Samocha KE, Banks E, Fennell T, et al. Analysis of protein-coding genetic variation in 60,706 humans. Nature. 2016;536(7616):285–91.
10. Fagerberg L, Hallstrom BM, Oksvold P, Kampf C, Djureinovic D, Odeberg J, et al. Analysis of the human tissue-specific expression by genome-wide integration of transcriptomics and antibody-based proteomics. Mol Cell Proteom. 2014;13(2):397–406.
11. Laurent A, Masse J, Omilli F, Deschamps S, Richard-Parpaillon L, Chartrain I, et al. ZFPIP/Zfp462 is maternally required for proper early Xenopus laevis development. Dev Biol. 2009;327(1):169–76.
12. Eberl HC, Spruijt CG, Kelstrup CD, Vermeulen M, Mann M. A map of general and specialized chromatin readers in mouse tissues generated by label-free interaction proteomics. Mol Cell. 2013;49(2):368–78.
13. Yelagandula R, Stecher K, Novatchkova M, Michetti L, Michlits G, Wang J, et al. ZFP462 safeguards neural lineage specification by targeting G9A/GLP-mediated heterochromatin to silence enhancers. Nat Cell Biol. 2023;25(1):42–55.
14. Masse J, Laurent A, Nicol B, Guerrier D, Pellerin I, Deschamps S. Involvement of ZFPIP/Zfp462 in chromatin integrity and survival of P19 pluripotent cells. Exp Cell Res. 2010;316(7):1190–201.
15. Wang B, Zheng Y, Shi H, Du X, Zhang Y, Wei B, et al. Zfp462 deficiency causes anxiety-like behaviors with excessive self-grooming in mice. Genes Brain Behav. 2017;16(2):296–307.
16. Hughes JR, Melyn M. EEG and seizures in autistic children and adolescents: further findings with therapeutic implications. Clin EEG Neurosci. 2005;36(1):15–20.
17. Xu CJ, Zhao XR, Zhang GZ, Li EZ, Wang J, Yang SH et al. EEG analysis of children with autism spectrum disorder and non epileptic mental retardation. Chin J Med. 2017;52(9):76–8.

Publisher's note